



Cite this: DOI: 10.1039/c6nj03908a

Bent-core mesogens with an aromatic unit at the terminal position†

 Kvetoslava Bajzиковá,^{id}^a Jiří Svoboda,^{id}^{*a} Vladimíra Novotná,^{id}^{*b}
 Damian Pocięcha^{id}^c and Ewa Gorecka^{id}^c
Received 13th December 2016,
Accepted 28th April 2017

DOI: 10.1039/c6nj03908a

rsc.li/njc

Bent-core liquid crystals with a naphthalene central unit and an aromatic ring at the terminal position of molecular tails were synthesised with the aim of enhancing nanosegregation. It was found that the length of the spacer between the rigid core and the terminal aromatic moiety had a profound influence on the liquid crystal polymorphism. The homologues with short spacers exhibited nematic and columnar phases, whereas the homologue with long spacers exhibited a tilted lamellar phase with a liquid-like in-plane order, indicating an unusual morphology of the densely packed toroidal objects. The morphology can be changed to twisted ribbons by small additives adsorbed on the membrane surface. This is the first example of twisted ribbons constructed by a lamellar system with no long-range in-plane order.

Introduction

The unusual properties of bent-core liquid crystals (BC) were first described in 1996;¹ since then, significant efforts have been devoted to establishing the molecular structure–mesomorphic property relationship for this group of materials. For bent-core mesogens, much richer polymorphism of mesophases has been observed as compared to rod-like molecules.² Besides the nematic phase, several smectic (lamellar) phases, mainly tilted smectic phases (SmCP) in which a close packing of the bent-core molecules results in a polar order, have been described and studied. The SmCP phases can be distinguished as antiferroelectric (A) and ferroelectric (F) according to their polar order and as synclinic (S) and anticlinic (A) according to the orientation of the tilt in the neighbouring layers.^{3,4} Bent-core mesogens can also form phases with a structure built of smectic layer fragments (columns) arranged into a 2D lattice; these columnar phases have been labelled as B₁-type.^{5,6} There are two general types of B₁ phases in which layer fragments are either directly connected to each other (B₁) or through a defect region (B_{1Rev});⁷ the phases differ in their electrooptical response: no switching is observed for B₁, whereas B_{1Rev} is usually sensitive to an applied electric field.

One of the most intriguing phases formed by bent-core molecules is the dark-conglomerate phase (DC).^{8–12} The DC phase is a smectic mesophase, but its texture is optically isotropic with optically active domains that are easily detectable *via* decrossing of the polarizers. It is generally accepted that the DC phase is formed from strongly deformed membranes (layer stacks) with local saddle-splay curvature (sponge morphology).¹³

Introduction of functional groups of various shapes and polarities into the terminal chains was utilized to enhance the nanosegregation and change the self-assembly process as well as the mesomorphic behaviour of the liquid crystalline materials.¹⁴ For example, in the field of rod-like mesogens, the bulky *tert*-butyl and cycloalkyl,^{15–19} alkylsilyl, oligosiloxane and carbosilane,^{15,19,20} semifluoroalkyl, polyfluoroalkyl, and aryl chains^{18–22} were introduced to tune the mesomorphic properties of the LCs. Few examples of benzene-terminated rod-like materials have also been investigated.^{19,23,24} Analogously, the role of different polar and bulky groups at the terminal position of the bent-core materials has been studied: *e.g.* linear alkyl, benzyl and perfluorophenyl esters,^{25–28} bulky adamantane,²⁹ fullerene,³⁰ alkylsilyl, oligosiloxane and carbosilane units,^{31–40} and semi- and polyfluorinated chains^{28,41–43} have been carefully investigated to recognize the structure–property relationship.

Herein, we report the synthesis and physical properties of a series of bent-core compounds terminated with an arylalkyl, heteroarylalkyl, and aryloxyalkyl chains. It was expected that the bulky aryl group at the terminal position should prevent interdigitation of the terminal chains between neighbouring layers, and the decoupled layers should be less stiff and therefore more susceptible to deformation. In addition, the compounds end-capped with a reactive aromatic and/or properly substituted aromatic group can be utilized in the future for the preparation of

^a Department of Organic Chemistry, University of Chemistry and Technology, CZ-166 28 Prague 6, Czech Republic. E-mail: Jiri.Svoboda@vscht.cz; Fax: +420 220444182; Tel: +420 220444288

^b Institute of Physics, Czech Academy of Sciences, Na Slovance 2, CZ-182 21 Prague 8, Czech Republic. E-mail: novotna@fzu.cz; Fax: +420 286890527; Tel: +420 266053111

^c Laboratory of Dielectrics and Magnetism, Chemistry Department, Warsaw University, Al. Zwirki i Wigury 101, 02-089 Warsaw, Poland. E-mail: pociu@chem.uw.edu.pl; Fax: +48 228221075; Tel: +48 228221075

† Electronic supplementary information (ESI) available. See DOI: 10.1039/c6nj03908a

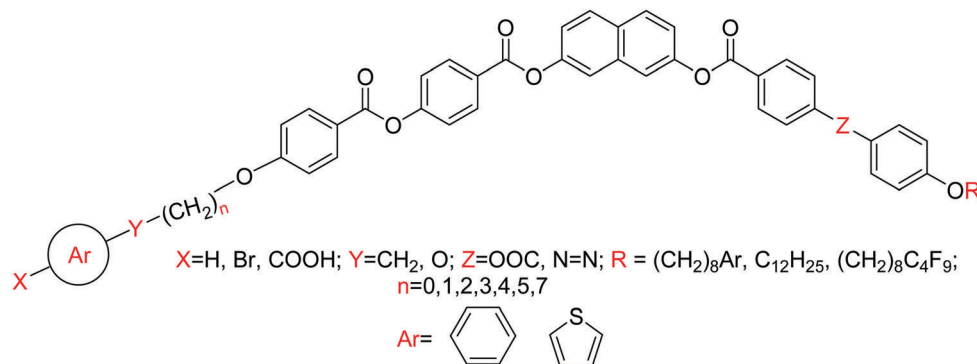


Fig. 1 General structure of the designed materials.

new types of metallic nanoparticles grafted with organometallic mesogenic ligands.^{44–46} To optimize the mesomorphic properties, the general molecular structure (Fig. 1) has been modified by changing the type of the linking group ($Z = \text{ester}$ and azo) in the lengthening arm, the length of the arylalkyl ($Y = \text{CH}_2$) and aryloxyalkyl ($Y = \text{O}$) terminal chains ($n = 0\text{--}5, 7$), the type of the aromatic unit ($Ar = \text{benzene}$ and thiophene), and the character of the terminal chain ($R = \text{alkyl}$, arylalkyl , and perfluoroalkyl).

For the design of new materials, we utilized our knowledge about the mesomorphic properties of the previously studied naphthalene-based mesogens.^{47–53} As a reference compound, we chose a material with two dodecyloxy terminal chains,⁴⁸ which was later modified by a nonafluorododecyloxy chain⁵³ and the outer ester linkage was also replaced by an azo moiety.⁵⁴ All these compounds exhibited SmCP type phases in a broad temperature range. For the compounds presented herein, the original dodecyl chain in the model compounds was primarily replaced by a phenyloctyl or 2-thienyloctyl unit to keep the length of the terminal chain unchanged. Furthermore, the second terminal alkyl chain R was also substituted by phenyloctyl or polyfluoroalkyl chains and the ester linkage Z was substituted by an azo group. Based on the preliminary results, the studied series was extended by modifying the length of the phenylalkyl chain (n), introduction of oxygen in the vicinity of the phenyl moiety ($Y = \text{O}$ and phenoxyalkyl), and phenyl substitution ($Br, COOH$).

Results and discussion

Experimental details are described in ESI.† For all the studied compounds, liquid crystalline phases were tentatively identified by their optical textures *via* a polarising microscope and confirmed by X-ray diffraction studies. The phase transitions and enthalpy changes were determined from the DSC measurements. DSC thermographs for the selected compounds from all series are presented in Fig. 2. Chemical formulae of the studied compounds are inserted into the headings of the corresponding tables.

Compounds of series **I** (Table 1) differ in the length of the linkage between the terminal phenyl ring and mesogenic core. A strong odd–even effect was observed regarding the clearing temperature and the phase sequence. For the materials **Ia**, **Ic**,

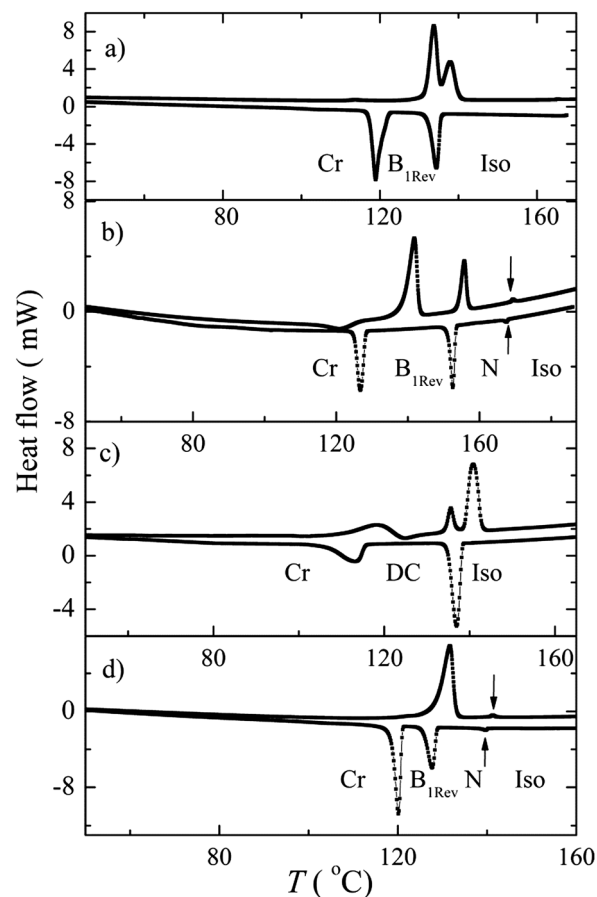


Fig. 2 DSC plots for selected compounds: (a) **Ib**, (b) **Ic**, (c) **If**, and (d) **Illa**, obtained during the second heating (upper) and cooling (lower curve) at a rate of 5 K min^{-1} . Arrows mark the phase transitions, which are not clearly seen at this scale; phases are indicated.

and **Ie** with an odd number of carbon atoms in the linkage, a sequence nematic–columnar phase was observed at rather high transition temperatures, whereas for the materials **Ib** and **Id** with an even number of carbon atoms, direct transition from the isotropic liquid to a columnar phase was found at substantially lower temperatures (Fig. 3). The nematic phase showed a typical marble-like texture⁵⁵ (Fig. 4a), whereas a mosaic texture was observed for the columnar phase (Fig. 4b). The columnar phase

Table 1 Phase transition temperatures, T_{tr} , in °C, and enthalpies, ΔH , in kJ mol⁻¹, were detected during the second cooling. Melting points, m.p., were obtained on the second heating. All thermographs were obtained at a rate of 5 K min⁻¹

Ia-f

| | n | m.p. (ΔH) | T_{cr} (ΔH) | M_2 | T_{tr} (ΔH) | M_1 | T_{tr} (ΔH) | Iso |
|-----------|-----|---------------------|-------------------------|-------------------|-------------------------|-------------------|-------------------------|-----|
| Ia | 1 | 171 (+27.7) | 146 (-28.1) | B _{1rev} | 168 (-10.7) | N | 181 (-0.3) | • |
| Ib | 2 | 132 (+12.1) | 121 (-16.5) | — | — | B _{1rev} | 136 (-11.0) | • |
| Ic | 3 | 139 (+30.1) | 128 (-14.6) | B _{1rev} | 153 (-10.9) | N | 168 (-0.4) | • |
| Id | 4 | 126 (+19.4) | 116 (-17.2) | — | — | B _{1rev} | 139 (-13.4) | • |
| Ie | 5 | 143 (+35.3) | 131 (-21.1) | B _{1rev} | 141 (-10.7) | N | 155 (-0.4) | • |
| If | 8 | 134 (+17.9) | 116 (-7.7) | — | — | DC | 138 (-12.6) | • |

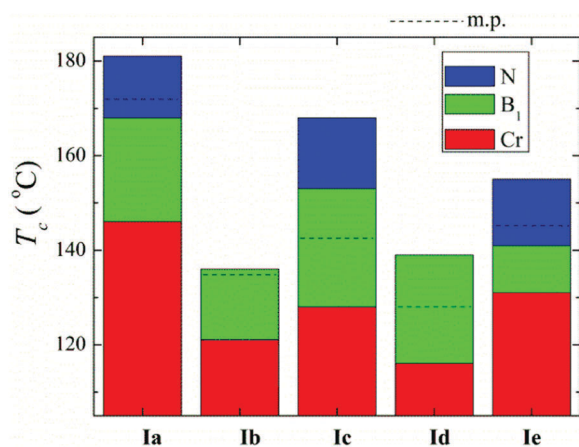


Fig. 3 Phase diagram for compounds **Ia–e**.

in all compounds, **Ia–Ie**, was identified as a broken-layer B_{1rev} type. Under an applied electric field, the B_{1rev} textures revealed changes in birefringence, but no switching of the extinction position was observed. For all the materials exhibiting the B_{1rev} phase, in the X-ray patterns, few incommensurate Bragg reflections were obtained at a low angle range and a diffused signal was observed in the high angle region (Fig. 5a). The best fitting of the signal positions was obtained *via* speculating an oblique 2D lattice (with $z = 2$). The crystallographic unit cell parameter b steadily increased by ~ 1 Å with elongation of the molecular arm by each methylene group (Table 2). Note that the parameter b is considerably smaller than the molecular length, suggesting that molecules in the layer fragments, forming the 2D columnar phase, are strongly tilted. The inclination angle of the crystallographic unit cell $\gamma \sim 100$ deg, as well as the sizes of the layer blocks (unit cell parameter $a \sim 28$ Å, corresponding to about 6 molecules in the block cross section) were only weakly dependent in the homologue series (Table 2). The speculated crystallographic lattice was confirmed by azimuthal signal positions in the 2D X-ray patterns for partially aligned samples. The ESI X-ray patterns, obtained for partially oriented

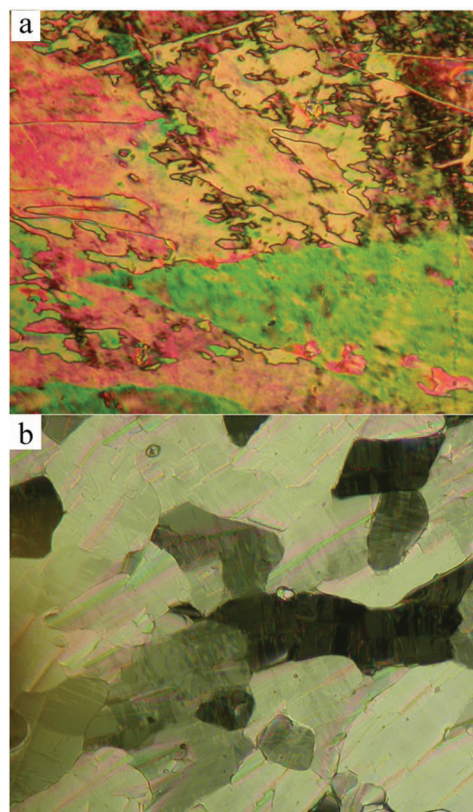


Fig. 4 Texture of **Ia** in (a) the nematic phase at $T = 172$ °C and (b) the columnar B₁ phase at $T = 164$ °C.

samples, are presented for different studied compounds (Fig. S1, ESI†).

For the longest studied homologue of series **I**, with $n = 8$ (**If**), another mesophase has been observed, with optical textures typical for a lamellar DC phase.^{8–12} The X-ray pattern confirmed the simple lamellar structure of the phase, and only commensurate peaks at low angle range were detected (Fig. 5b). The layer thickness determined from the signal position was much smaller than the

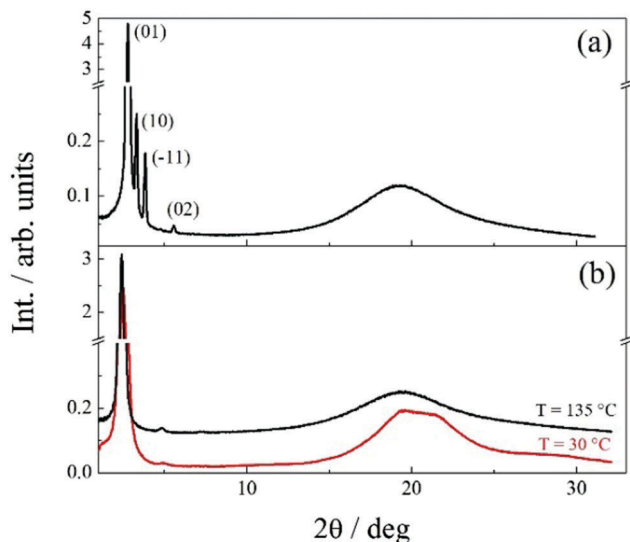


Fig. 5 X-ray patterns for the compounds (a) **Id** in the B_{1rev} phase and (b) **If** in the DC phase ($T = 135$ °C) and glassy state of the DC phase ($T = 30$ °C).

molecular length, suggesting tilted arrangement of the molecules in the layers (tilt angle ~ 40 – 45 deg). In the high diffraction angle region, a diffused maximum corresponding to an average distance between molecules was present, typical for LC mesophases with short-range molecular ordering in the layers. Optical textures of the lamellar phase evidenced nearly zero birefringence, indicating that the orientation of the molecules in the phase was space-averaged over distances smaller than the wavelength of visible light; however, the textures show large (micron-size) optically active domains with right- and left-handed optical rotatory power (Fig. 6), characteristic for dark-conglomerate (DC) phase.^{8–12} The optical activity was nearly temperature independent, ~ 0.25 degree per μm . The application of an electric field induced a reversible change to the birefringent grainy texture. Apparently, the electric field straightened the layers. Rapid cooling of the sample did not change the texture, and the boundaries of the optically active domains were preserved. The X-ray pattern of the temperature-quenched sample, obtained at room temperature, shows that the high angle signal is broad although weakly split, evidencing the glassy state of the DC phase, with short positional correlations inside the layers. Temperature quenching of the sample prevents recrystallization, and the sample remains in the DC phase.

To obtain some insight into the nature of the DC phase, its morphology was investigated *via* AFM (Fig. 7). The AFM images obtained for thermally quenched samples revealed characteristic, densely packed toroidal-like objects with the diameter ~ 150 – 250 nm, built of 4–5 short, connected tubules with the diameter ~ 50 – 80 nm, and the tubules were made of wrapped layers. At higher magnification (Fig. 7b), it was possible to detect that the central part of the torus was filled with cylindrically folded layers. The morphology of the DC phase resembles focal conic domains, interconnected in 3D space. It was recently shown that the morphology of the lamellar crystals (B_4 phase) can be changed in the presence of some additives in the system.⁵⁶ Moreover, for

Table 2 Cell parameters measured by X-ray for selected compounds at temperatures T

| $T/^\circ\text{C}$ | $a/\text{\AA}$ | $c/\text{\AA}$ | $\beta/^\circ$ |
|--------------------|----------------|----------------|----------------|
| Ia | | | |
| 165 | 25.6 | 30.0 | 103.8 |
| Ib | | | |
| 133 | 26.9 | 30.9 | 104.4 |
| Ic | | | |
| 148 | 28.3 | 31.6 | 103.4 |
| 140 | 28.2 | 31.7 | 103.6 |
| 130 | 28.3 | 31.7 | 103.8 |
| Id | | | |
| 135 | 27.1 | 32.7 | 102.4 |
| 125 | 27.4 | 32.7 | 102.3 |
| Ie | | | |
| 137 | 28.8 | 33.1 | 103.0 |
| If | | | |
| 135 | $d = 36.4$ | | |
| 130 | $d = 36.4$ | | |
| 125 | $d = 36.3$ | | |
| Ila | | | |
| 180 | 29.1 | 40.2 | 92.3 |
| Ild | | | |
| 150 | $d = 38.8$ | | |
| 130 | $d = 38.3$ | | |
| IIf | | | |
| 135 | $d = 36.1$ | | |
| Ilg | | | |
| 145 | $d = 38.9$ | | |
| IIc | | | |
| 120 | 24.9 | 40.5 | 89.1 |

the studied materials, doping with a small amount of nematic compound (~ 10 wt% of 6CHBT, see Fig. S5, ESI†) influenced the sample morphology. In mixtures, the toroidal-like objects were replaced with irregular sponge with some twisted ribbons (Fig. 7c and Fig. S6, ESI†), similar to those found in the B_4 phase.⁵⁷ The X-ray studies showed that although the morphology of the system changed, the crystallographic structure of the DC phase remained unchanged under doping, the layer thickness only slightly expanded (by a few% in ~ 20 wt% mixture), and the in-plane order stayed short-range. This clearly shows that despite the liquid crystalline smectic order of the DC phase, the components of the mixture segregate at nanoscale, and only a very limited number of nematogenic molecules are incorporated in the membranes of the dark conglomerate phase and most probably in the regions between smectic layers. This finding is contrary to the common behaviour of the LC mixtures, for which it was observed that even chemically different mesogenic molecules (rod and bent-core) can form homogeneous smectic structures with the layer thickness linearly related to the mixture concentration.⁵⁸ For the studied system, demixing of the materials was observed despite the fact that the membranes were built of layers having liquid like in-plane order. It seems

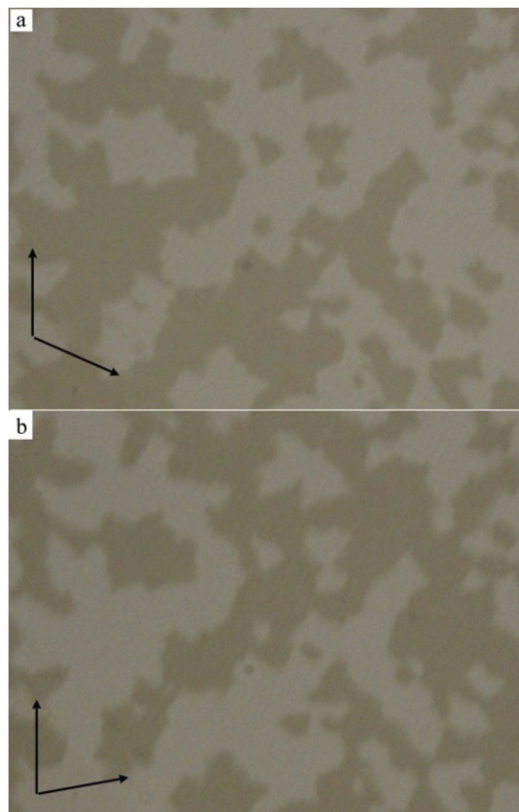


Fig. 6 Texture of **If** observed using a polarizing microscope; polarizers are de-crossed by an angle of about 6 degrees (a) clockwise and (b) anticlockwise. The position of polarizers is schematically depicted and the width of the image corresponds to 150 μm .

that the formation of toroidal or twisted nanofilament objects does not require crystalline layers, like in the B_4 phase.⁵⁸ Moreover, all morphologies (toroidal, sponge, and twisted ribbons) are driven by the same tendency towards saddle-splay deformation of membranes. The energy balance between different morphologies is rather subtle and might be changed *via* the adsorption of the dopant molecules on the membrane surface or *via* weakening of the layer coupling. In both cases, the toroidal objects are replaced by objects, such as membranes or ribbons, with higher surface to volume ratio.

Molecular structures with the shortest and longest linkages between the terminal aryl ring and mesogenic core ($n = 1$ and $n = 8$, respectively) were subjected to further modifications, see Table 3. Exchanging of the alkyl terminal chain by a partially fluorinated chain of the same length (compounds **IIa** and **IIc**) resulted in an increase of the clearing temperature by ~ 20 K, and the phase sequence was not affected. Replacement of an ester linkage at the *Z* position in the molecular arm (Table 3) with an azo moiety (compounds **IIb** and **IIe**) caused an increase in the melting temperature; this prevented observation of the columnar phase in **IIb** and resulted in a change in the liquid crystalline phase in the case of compound **IIe** – columnar phase was found instead of the DC lamellar phase formed by an analogous compound **If**.

Additionally, another type of aryl ring at the terminal position was tested; for materials **IIf–h**, a thiophene unit was applied.

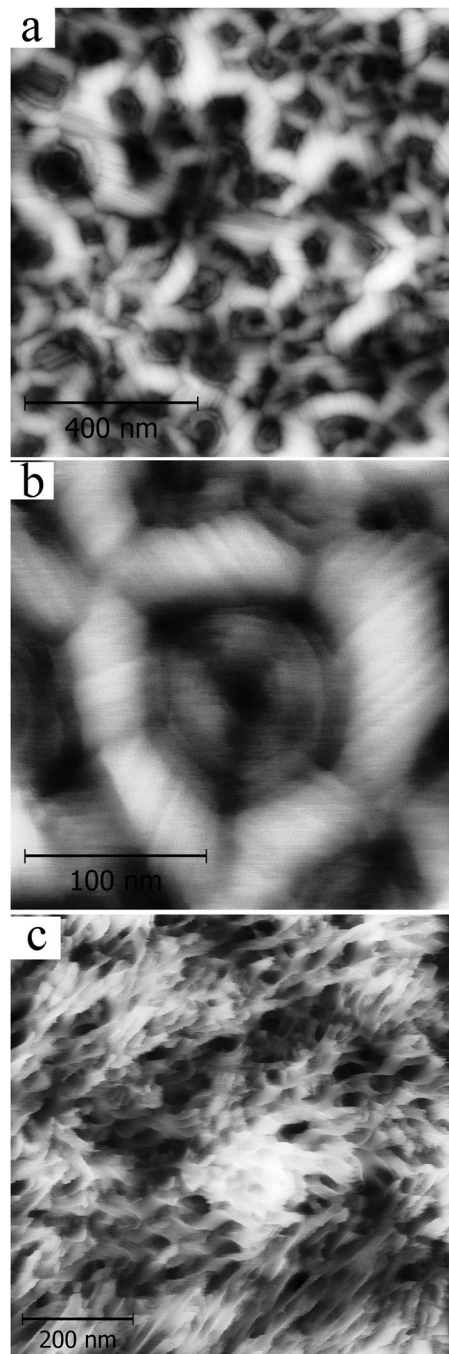
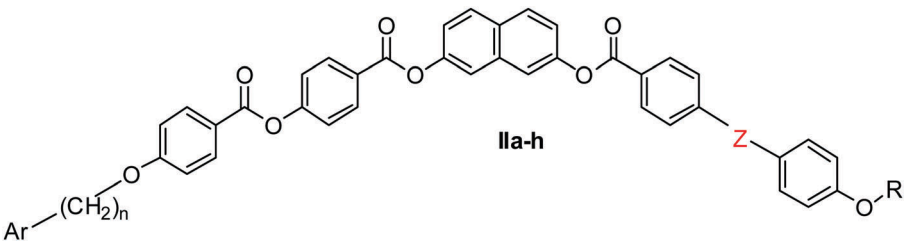


Fig. 7 AFM images: (a and b) for compound **If** obtained at room temperature for a sample quenched from the DC phase (figures differing in resolution); (c) for mixture of compound **If** with 10 wt% of nematogen 6CHB; twisted ribbons are clearly visible in the left part of the image.

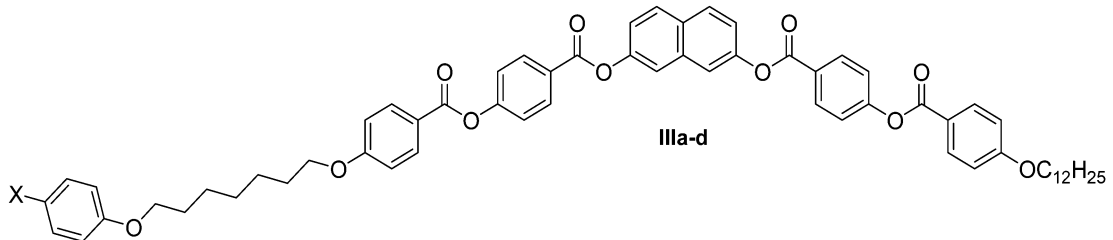
Although the presence of sulphur in the thiophene ring introduced an additional dipole moment (~ 0.5 D), mesomorphic properties of the materials **IIf–g** were similar to their analogues with a phenyl ring in the terminal chain. Only in the case of the azo derivative **IIh**, there was a change in the type of LC phase formed; the nematic phase was observed instead of the columnar phase found in **IIe**. Material **IIc**, in which phenyl rings were applied at the ends of both terminal chains, showed no liquid crystalline phases.

Table 3 Phase transition temperatures, T_{tr} , and temperature of crystallization, T_{cr} , in °C detected during the second cooling, and the corresponding enthalpies, ΔH , are in brackets in kJ mol^{-1} . Melting points, m.p., have been obtained during the second heating. All thermographs were obtained at a rate of 5 K min^{-1} . Ph = phenyl, Th = 2-thienyl



| | n | Z | Ar | R | m.p. (ΔH) | T_{cr} (ΔH) | M_2 | T_{cr} (ΔH) | M_1 | T_{tr} (ΔH) | Iso |
|------------|-----|-----|----|---------------------------------------|---------------------|-------------------------|------------|-------------------------|------------|-------------------------|-----|
| IIa | 1 | OOC | Ph | $(\text{CH}_2)_8\text{C}_4\text{F}_9$ | 192 (+43.2) | 177 (-35.1) | B_{1Rev} | 189 (-8.6) | N | 202 (-0.6) | • |
| IIb | 1 | N=N | Ph | $\text{C}_{12}\text{H}_{25}$ | 182 (+56.2) | 176 (-52.3) | — | — | N | 188 (-0.4) | • |
| IIc | 8 | OOC | Ph | $(\text{CH}_2)_8\text{Ph}$ | 123 (+25.4) | 113 (-25.3) | — | — | — | — | • |
| IId | 8 | OOC | Ph | $(\text{CH}_2)_8\text{C}_4\text{F}_9$ | 140 (+22.2) | 118 (-21.0) | — | — | DC | 161 (-13.5) | • |
| IIe | 8 | N=N | Ph | $\text{C}_{12}\text{H}_{25}$ | 148 (+31.7) | 135 (-20.4) | — | — | B_{1Rev} | 139 (-9.5) | • |
| IIf | 8 | OOC | Th | $\text{C}_{12}\text{H}_{25}$ | 120 (+22.1) | 119 (-10.1) | — | — | DC | 139 (-15.2) | • |
| IIg | 8 | OOC | Th | $(\text{CH}_2)_8\text{C}_4\text{F}_9$ | 142 (+74.7) | 121 (-68.1) | — | — | DC | 157 (-15.1) | • |
| IIh | 8 | N=N | Th | $\text{C}_{12}\text{H}_{25}$ | 146 (+35.2) | 132 (-17.3) | — | — | N | 138 (-6.7) | • |

Table 4 Phase transition temperatures, T_{tr} , in °C, and enthalpies, ΔH , in kJ mol^{-1} , were obtained during the second cooling. Melting points, m.p., were obtained during the second heating. All thermographs were obtained at a rate of 5 K min^{-1}



| | X | m.p. (ΔH) | T_{cr} (ΔH) | M_2 | T_{tr} (ΔH) | M_1 | T_{tr} (ΔH) | Iso |
|-------------|---------------------------|---------------------|-------------------------|------------|-------------------------|-------|-------------------------|-----|
| IIIa | H | 128 (+27.9) | 121 (-16.8) | B_{1Rev} | 129 (-9.4) | N | 140 (-0.3) | • |
| IIIb | Br | 130 (+33.4) | 116 (-19.2) | B_{1Rev} | 127 (-6.4) | N | 155 (-0.4) | • |
| IIIc | PhCH_2OOC | 111 (+17.1) | 104 (-14.7) | B_{1Rev} | 121 (-8.3) | N | 127 (-0.5) | • |
| IIId | HOOC | 195 (+11.9) | 171 (-24.1) | — | — | — | — | • |

All materials forming the DC phase had morphologies similar to those observed for the **If** compound, *i.e.* densely packed toroidal objects were visible in their AFM images.

Finally, a methylene group in the vicinity of the terminal phenyl group was substituted for oxygen in the materials **III** (Table 4). In addition, some functionality was introduced into the phenyl ring, which could be utilized in the planned design of the organometallic ligands. In comparison with **If**, the presence of oxygen and thus formation of an additional dipole in the terminal chain of **IIIa** resulted in a change of mesomorphic behaviour and a sequence of N- B_{1Rev} phases was observed. The transition was strongly first order; therefore, as expected, only weak cybotactic groups were observed in the nematic phase *via* the X-ray method (Fig. S2, ESI[†]). Moreover, similar observation was obtained for the bromophenyl substituted material **IIIb**. Compound **IIIc**, although having a bulky group in the terminal position, exhibits the mesomorphic behaviour. On the other hand, material **IIId** with a free carboxylic group, which can easily

form strong hydrogen bonds, is not mesogenic. Mesophases formed by the compounds of series **III** exhibit typical optical textures, and examples are presented in ESI[†] (Fig. S3 for **IIIb**). The B_{1Rev} phase show characteristic colour domains, which do not reveal any electrooptical response. Crystallographic unit cell parameters for the selected compounds of series **II** and **III** are presented in Table 2.

Conclusions

The bent-core compounds with an aromatic and/or substituted aromatic unit placed at the end of the terminal chain, exhibiting nematic-columnar phase sequence, were prepared and studied. A strong even-odd effect was observed with respect to the length of the alkyl linkage in the terminal chain, which was much more pronounced compared to that of the previously studied bent-core compounds with simple alkyl/alkoxy terminal chains. It is evident

that the alkyl chain terminated by a phenyl ring adopts a different conformation depending on the parity of the chain. While the phenyl ring retains the linear arrangement for the even number of atoms in the linkage, for the odd-numbered chains, the phenyl ring deviates from linearity, which influences the process of self-assembly and therefore isotropization temperatures. Surprisingly, crystallographic lattice parameters of the columnar B_{1rev} phase are very similar for all homologues, regardless of the chain length and parity.

For long terminal arylalkyl chains, the studied compounds formed the DC phase. Similar tendency towards the lamellar phases upon elongation of the terminal chain has been observed for the previously studied dodecyl substituted analogue.⁴⁸ It could be concluded that the bulky moiety at the terminal position of the bent-core mesogens prevents interdigitation of the molecules between adjacent layers, and thus, the decoupled layers are more susceptible to deformations. The studied materials form either broken layer columnar phases or a lamellar phase with complex morphology (DC phase) driven by a tendency towards saddle-splay deformation. In the DC phase of pure material, the interconnected toroidal objects are formed and the morphology can be changed by adding small amount of nematogenic molecules. Then, the toroidal objects are replaced by sponge or twisted ribbons, without changes in the smectic layer structure. Previously, the formation of twisted ribbons or toroidal objects was observed for the lamellar crystal phase (B₄),⁵⁷ whereas the phase with soft smectic layers (DC phase) displayed random network of curved membranes.⁸⁻¹²

Acknowledgements

This project was supported by the Czech Science Foundation (projects No. 15-02843S and 16-12150S).

References

- 1 T. Niori, T. Sekine, J. Watanabe, T. Furukawa and H. Takezoe, *J. Mater. Chem.*, 1996, **6**, 1231.
- 2 G. Pelzl, S. Diele and W. Weissflog, *Adv. Mater.*, 1999, **11**, 707, and references cited therein.
- 3 D. A. Coleman, J. Fernsler, N. Chattham, M. Nakata, Y. Takanishi, E. Körblova, D. R. Link, R.-F. Shao, W. G. Jang, J. E. MacLennan, O. Mondain-Monval, C. Boyer, W. Weissflog, G. Pelzl, L.-C. Chien, J. Zasadzinski, J. Watanabe, D. M. Walba, H. Takezoe and N. A. Clark, *Science*, 2003, **301**, 1204.
- 4 R. Amarantha Reddy and C. Tschierske, *J. Mater. Chem.*, 2006, **16**, 907.
- 5 J. Szydłowska, J. Mieczkowski, J. Matraszek, D. W. Bruce, E. Gorecka, D. Pociecha and D. Guillon, *Phys. Rev. E: Stat., Nonlinear, Soft Matter Phys.*, 2003, **67**, 031702.
- 6 E. Gorecka, N. Vaupotic and D. Pociecha, *Chem. Mater.*, 2007, **19**, 3027.
- 7 M. Kohout, J. Tůma, J. Svoboda, V. Novotná, E. Gorecka and D. Pociecha, *J. Mater. Chem. C*, 2013, **1**, 4962.
- 8 H. Ocak, B. Bilgin-Eran, M. Prehm and C. Tschierske, *Soft Matter*, 2013, **9**, 4590.
- 9 A. Roy, M. Gupta, S. Radhika, B. K. Sadashiva and R. Pratibha, *Soft Matter*, 2012, **8**, 7207.
- 10 M. Alaasar, M. Prehm, M. Brautzsch and C. Tschierske, *J. Mater. Chem. C*, 2014, **2**, 5487.
- 11 M. Nagaraj, K. Usami, Z. Zhang, V. Görtz, J. W. Goodby and H. F. Gleeson, *Liq. Cryst.*, 2014, **41**, 800.
- 12 L. E. Hough, M. Spanneth, M. Nakata, D. A. Coleman, C. D. Jones, G. Dantlgraber, C. Tschierske, J. Watanabe, E. Körblova, D. M. Walba, J. E. MacLennan, M. A. Glaser and N. A. Clark, *Science*, 2009, **325**, 452.
- 13 M. Nagaraj, J. C. Jones, V. P. Panov, H. Liu, G. Portale, W. Bras and H. F. Gleeson, *Phys. Rev. E: Stat., Nonlinear, Soft Matter Phys.*, 2015, **91**, 042504.
- 14 N. Gimeno and M. Blanca Ros, in *Handbook of Liquid Crystals*, ed. J. W. Goodby, P. J. Collings, T. Kato, C. Tschierske, H. F. Gleeson, P. Raynes, Wiley-VCH, Weinheim, 2014, vol. 4, pp. 603–679, and references cited therein.
- 15 I. A. Radini and M. Hird, *Liq. Cryst.*, 2009, **36**, 1417.
- 16 S. J. Cowling, A. W. Hall and J. W. Goodby, *Liq. Cryst.*, 2005, **32**, 1483.
- 17 S. J. Cowling, A. W. Hall and J. W. Goodby, *Adv. Mater.*, 2005, **17**, 1077.
- 18 S. J. Cowling, A. W. Hall and J. W. Goodby, *J. Mater. Chem.*, 2011, **21**, 9031.
- 19 J. W. Goodby, I. M. Saez, S. J. Cowling, J. S. Gasowka, R. A. MacDonald, S. Sia, P. Watson, K. J. Toyne, M. Hird, R. A. Lewis, S.-E. Lee and V. Vashchenko, *Liq. Cryst.*, 2009, **36**, 567.
- 20 R. J. Mandle, E. J. Davis, C.-C. A. Voll, D. J. Daniel, S. J. Cowling and J. W. Goodby, *J. Mater. Chem. C*, 2015, **3**, 2380.
- 21 S. V. Arehart and C. Pugh, *J. Am. Chem. Soc.*, 1997, **119**, 3027.
- 22 Y.-G. Yang, H. Li and J. Wen, *Liq. Cryst.*, 2007, **34**, 1167.
- 23 I. Nishiyama, T. Yamamoto, J. Yamamoto, J. W. Goodby and H. Yokoyama, *J. Mater. Chem.*, 2003, **13**, 1868.
- 24 I. Nishiyama, T. Yamamoto, J. Yamamoto, H. Yokoyama and J. W. Goodby, *Mol. Cryst. Liq. Cryst.*, 2005, **439**, 55.
- 25 J. P. Bedel, J. C. Rouillon, J. P. Marcerou, M. Laguerre, H. T. Nguyen and M. F. Achard, *Liq. Cryst.*, 2001, **28**, 1285.
- 26 J. P. Bedel, J. C. Rouillon, J. P. Marcerou, H. T. Nguyen and M. F. Achard, *Phys. Rev. E: Stat., Nonlinear, Soft Matter Phys.*, 2004, **69**, 061702.
- 27 G. Pelzl, M. G. Tamba, S. Findeisen-Tandel, M. W. Schröder, U. Baumeister, S. Diele and W. Weissflog, *J. Mater. Chem.*, 2008, **18**, 3017.
- 28 D. Kardas, M. Prehm, U. Baumeister, D. Pociecha, R. Amarantha Reddy, G. H. Mehl and C. Tschierske, *J. Mater. Chem.*, 2005, **15**, 1722.
- 29 A. Jáklí, I. C. Pintre, J. L. Serrano, M. Blanca Ros and M. R. de la Fuente, *Adv. Mater.*, 2009, **21**, 3784.
- 30 J. Vergara, J. Barberá, J. L. Serrano, M. Blanca Ros, N. Sebastián, R. de la Fuente, D. O. López, G. Fernández, L. Sánchez and N. Martín, *Angew. Chem., Int. Ed.*, 2011, **50**, 12523.
- 31 C. Keith, R. Amarantha Reddy, A. Hauser, U. Baumeister and C. Tschierske, *J. Am. Chem. Soc.*, 2006, **128**, 3051.
- 32 R. Achten, A. Koudijs, M. Giesbers, R. Amarantha Reddy, T. Verhulst, C. Tschierske, A. T. M. Marcelis and E. J. R. Sudhölter, *Liq. Cryst.*, 2006, **33**, 681.

- 33 R. Amarantha Reddy, U. Baumeister, J. L. Chao, H. Kresse and C. Tschierske, *Soft Matter*, 2010, **6**, 3883.
- 34 G. Dantlgraber, A. Eremin, S. Diele, A. Hauser, H. Kresse, G. Pelzl and C. Tschierske, *Angew. Chem., Int. Ed.*, 2002, **41**, 2408.
- 35 C. Keith, R. Amarantha Reddy, U. Baumeister and C. Tschierske, *J. Am. Chem. Soc.*, 2004, **126**, 14312.
- 36 Y. Zhang, M. J. O'Callaghan, U. Baumeister and C. Tschierske, *Angew. Chem., Int. Ed.*, 2008, **47**, 6892.
- 37 R. Amarantha Reddy, U. Baumeister and C. Tschierske, *Chem. Commun.*, 2009, 4236.
- 38 C. L. Folcia, J. Ortega, J. Etxebarria, S. Rodriguez-Conde, G. Sanz-Enfuita, K. Geese, C. Tschierske, V. Ponsinet, P. Barois, R. Pindak, L. D. Pan, Z. Q. Liu, B. K. McCoy and C. C. Huang, *Soft Matter*, 2014, **10**, 196.
- 39 Y. Zhang, U. Baumeister, C. Tschierske, M. J. O'Callaghan and C. Walker, *Chem. Mater.*, 2010, **22**, 2869.
- 40 C. Zhu, C. Shao, R. Amarantha Reddy, D. Chen, Y. Shen, T. Gong, M. A. Glaser, E. Korblova, P. Rudquist, J. E. MacLennan, D. M. Walba and N. A. Clark, *J. Am. Chem. Soc.*, 2012, **134**, 9681.
- 41 D. Shen, A. Pegenau, S. Diele, I. Wirth and C. Tschierske, *J. Am. Chem. Soc.*, 2000, **122**, 1593.
- 42 L. Kovalenko, W. Weissflog, S. Grande, S. Diele, G. Pelzl and I. Wirth, *Liq. Cryst.*, 2000, **27**, 683.
- 43 A. Kovářová, J. Svoboda, V. Kozmík, V. Novotná, M. Glogarová and D. Pocięcha, *Liq. Cryst.*, 2012, **32**, 755.
- 44 Z.-L. Cheng, R. Skouta, H. Vazquez, J. R. Widawsky, S. Schneebeli, W. Chen, M. S. Hybertsen, R. Breslow and L. Venkataraman, *Nat. Nanotechnol.*, 2012, **7**, 663.
- 45 D. Khobragade, E. S. Stensrud, M. Mucha, J. R. Smith, R. Pohl, I. Stibor and J. Michl, *Langmuir*, 2010, **26**, 8483.
- 46 E. Kaletova, A. Kohutova, J. Hajduch, J. Kaleta, Z. Bastl, L. Pospíšil, I. Stibor, T. F. Magnera and J. Michl, *J. Am. Chem. Soc.*, 2015, **137**, 12086.
- 47 J. Svoboda, V. Novotná, V. Kozmík, M. Glogarová, W. Weissflog, S. Diele and G. Pelzl, *J. Mater. Chem.*, 2003, **13**, 2104.
- 48 V. Kozmík, M. Kuchař, J. Svoboda, V. Novotná, M. Glogarová, U. Baumeister and S. Diele, *Liq. Cryst.*, 2005, **32**, 1151.
- 49 V. Kozmík, A. Kovářová, M. Kuchař, J. Svoboda, V. Novotná, M. Glogarová and J. Kroupa, *Liq. Cryst.*, 2006, **33**, 41.
- 50 V. Novotná, J. Žurek, V. Kozmík, J. Svoboda and M. Glogarová, *Liq. Cryst.*, 2008, **35**, 1023.
- 51 W. Weissflog, G. Pelzl, H. Kresse, U. Baumeister, K. Brand, M. W. Schröder, M. B. Tamba, S. Findeisen-Tandel, U. Kornek, S. Stern, A. Eremin, R. Stannarius and J. Svoboda, *J. Mater. Chem.*, 2010, **20**, 6057.
- 52 V. Kozmík, P. Polášek, A. Seidler, M. Kohout, J. Svoboda, V. Novotná, M. Glogarová and D. Pocięcha, *J. Mater. Chem.*, 2010, **20**, 7430.
- 53 A. Kovářová, V. Kozmík, J. Svoboda, V. Novotná, M. Glogarová and D. Pocięcha, *Liq. Cryst.*, 2012, **39**, 755.
- 54 J. Svoboda, unpublished results.
- 55 I. Dierking, *Textures of Liquid Crystals*, Wiley-VCH, Weinheim, 2003.
- 56 E. Gorecka, N. Vaupotić, A. Zep and D. Pocięcha, *Angew. Chem., Int. Ed.*, 2016, **55**, 12238.
- 57 J. Matraszek, N. Topnani, N. Vaupotić, H. Takezoe, J. Mieczkowski, D. Pocięcha and E. Gorecka, *Angew. Chem., Int. Ed.*, 2016, **55**, 3468.
- 58 A. Zep, K. Sitkowska, D. Pocięcha and E. Gorecka, *J. Mater. Chem. C*, 2014, **2**, 2323.